

# MEF2A is a transcription factor for circPVT1 and contributes to the malignancy of acute myeloid leukemia

KUN WU<sup>1,2\*</sup>, YUNTAO LI<sup>3\*</sup>, BO NIE<sup>3</sup>, CHONG GUO<sup>1,2</sup>, XIAOBO MA<sup>1,2</sup>, LINYAN LI<sup>1,2</sup>, SHENJU CHENG<sup>1,2</sup>, YANHONG LI<sup>1,2</sup>, SHAN LUO<sup>1,2</sup>, YUN ZENG<sup>3</sup>, JIAN YU<sup>4</sup> and MINGXIA SHI<sup>3</sup>

<sup>1</sup>Yunnan Key Laboratory of Laboratory Medicine, Clinical Research Center for Laboratory Medicine, Kunming, Yunnan 650032, P.R. China; <sup>2</sup>Department of Clinical Laboratory, The First Affiliated Hospital of Kunming Medical University, Kunming, Yunnan 650032, P.R. China; <sup>3</sup>Department of Hematology, Hematology Research Center of Yunnan Province, The First Affiliated Hospital of Kunming Medical University, Kunming, Yunnan 650032, P.R. China; <sup>4</sup>Interdisciplinary Institute for Cancer Diagnosis and Treatment, Beijing Advanced Innovation Center for Biomedical Engineering, Beihang University, Beijing 100083, P.R. China

Received June 3, 2024; Accepted September 9, 2024

DOI: 10.3892/ijo.2024.5699

**Abstract.** Acute myeloid leukemia (AML) is a hematological malignancy with a high relapse rate and a poor survival rate. The circular RNA circPVT1 and myocyte enhancer factor 2A (MEF2A) have unique functions in the progression of AML; however, the underlying mechanisms and clinical significance remain to be clarified. Bioinformatics and database analyses were used to assess the transcription factors and target genes of circPVT1. Dual-luciferase reporter gene and argonaute 2-RNA immunoprecipitation assays were used to verify the targeted relationships. The expression levels of related genes and proteins were detected by reverse transcription-quantitative PCR and western blotting. Cell viability and apoptosis were detected by Cell Counting Kit-8 assay and flow cytometry, respectively. The results revealed that circPVT1 was highly expressed in AML samples and cell lines, and that MEF2A regulated the expression of circPVT1. MEF2A overexpression promoted cell viability and epithelial-mesenchymal transition (EMT), and inhibited cell apoptosis. In addition, circPVT1 was revealed to target the regulation of microRNA (miR)-455-3p,

and miR-455-3p targeted the regulation of MCL1 expression, thus indicating that circPVT1 promoted MCL1 expression through its interaction with miR-455-3p. Furthermore, cells were transfected with the small interfering RNA-(si)-circPVT1, miR-455-3p inhibitor or si-MCL1, and si-circPVT1 and si-MCL1 inhibited the viability and EMT of NB4 and HL-60 cells. However, the miR-455-3p inhibitor had the opposite effect on cells. In conclusion, MEF2A may act as a transcription factor of circPVT1 to promote the malignant process of AML, and knockdown of circPVT1 could inhibit the viability and EMT of AML cells through the miR-455-3p/MCL1 axis.

## Introduction

Acute myeloid leukemia (AML) is a hematological malignancy of myeloid cells and is the most common type of leukemia in adults (1). AML is characterized mainly by the clonal proliferation of myeloid precursors and genetic abnormalities of cell components, such as chromosomal alterations and genetic mutations (2,3), and predominantly exhibits single lineage dysplasia; however, blasts from patients are heterogeneous for the antigens expressed (4,5). Leukemia is associated with genomic instability and clonal heterogeneity; the heterogeneity includes differences in tumor cell morphology, cell surface markers and functional characteristics (6). The etiology of most AML cases is currently unclear, but a number of risk factors exist (7). Moreover, the morbidity of AML has been reported to be increasing annually, the mortality rate remains high and treatment efficacy is poor. Notably, the global 5-year survival rate of AML is <50% (8,9). Therefore, it is necessary to clarify the molecular pathogenesis of AML and to identify potential therapeutic strategies.

Circular RNAs (circRNAs) are novel and extensive noncoding RNAs that regulate key functions in different types of cancer. The heterogeneity of circRNAs in tissues contributes to cell transformation and the development of numerous diseases, promotes the occurrence of tumors, and is a molecular biomarker and intervention target for the clinical diagnosis, treatment and prognosis of various types of cancer, including

---

*Correspondence to:* Dr Mingxia Shi, Department of Hematology, Hematology Research Center of Yunnan Province, The First Affiliated Hospital of Kunming Medical University, 295 Xichang Road, Kunming, Yunnan 650032, P.R. China  
E-mail: shmxia2002@sina.com

Dr Jian Yu, Interdisciplinary Institute for Cancer Diagnosis and Treatment, Beijing Advanced Innovation Center for Biomedical Engineering, Beihang University, 37 Xueyuan Road, Haidian, Beijing 100083, P.R. China  
E mail: yulab@buaa.edu.cn

\*Contributed equally

**Key words:** acute myeloid leukemia, myocyte enhancer factor 2A, circPVT1, microRNA-455-3p, MCL1

colorectal cancer, AML, hepatocellular carcinoma and gastric carcinoma (10-12). circRNA\_0016624 and circHIPK3 have been shown to mediate the related mechanisms of osteoblasts and osteoporotic cells, and serve as new therapeutic targets for osteoporosis (13). Researchers studying preeclampsia have successfully identified several circRNAs that may be used as promising biomarkers for the prediction and diagnosis of this disease (14). Furthermore, previous studies have shown that circRNA imbalance occurs in a variety of tumors. In gastric cancer, circPVT1 (15), circLARP4 (16), hsa-circ-0000096 (17) and circ-100269 (18) have been shown to promote tumor growth. Among the different circRNAs involved in cancer, circPVT1 has been reported to exhibit important carcinogenic features in multiple types of cancer. Notably, circPVT1 can promote the development of osteosarcoma by regulating the microRNA (miRNA/miR)-205-5p/c-FLIP axis (19). Abnormal expression of circPVT1 has also been shown to participate in the chemoresistance of lung adenocarcinoma by regulating the miR-145-5p/ABCC1 axis (20). Another study reported that circPVT1 is highly expressed in breast cancer tissues and cells, and inhibition of circPVT1 expression can significantly inhibit the proliferation and epithelial-mesenchymal transition (EMT) of breast cancer cells, and promote cell apoptosis (21). In addition, circPVT1 has been suggested to be carcinogenic in AML (22). However, there are few reports (23,24) on the specific molecular mechanisms underlying the effects of circPVT1 on AML progression. Therefore, the present study aimed to further explore the function of circPVT1, in order to provide potential molecular targets for the treatment of AML.

A number of studies have shown that the abnormal expression or mutation of the muscle cell enhancer factor 2 (MEF2) family (MEF2A, MEF2B, MEF2C and MEF2D) is inextricably linked with cancer, including large B-cell lymphoma (25) leukemia (26), and the solid tumors liver cancer (27) and colorectal cancer (28). MEF2A, as a transcription factor, can regulate the expression of various genes, thereby affecting the cancer process. A previous study reported that MEF2A binds to the lncHCP5 promoter region, promotes lncHCP5 expression and affects the progression of gastric cancer (29). MEF2A can also promote colorectal cancer progression by upregulating the expression of ZEB2 and CTNNB1 (30). Another study reported that MEF2A and MEF2D could regulate pancreatic cancer progression by controlling transcription of FNIP1 and FNIP2 (31). These findings suggested that MEF2A may serve an important regulatory role in cancer progression. In addition, our research group analyzed the promoter binding site of circPVT1 and found that the transcription factor MEF2A can bind the promoter region of circPVT1 with a high affinity. However, the mechanism by which MEF2A acts as a transcription factor for circPVT1 in AML progression is not yet clear; thus, the present study may provide an opportunity to develop new AML therapeutic strategies involving MEF2A as a transcription factor for circPVT1.

A number of studies have shown that circRNAs participate in the competitive endogenous RNA (ceRNA) mechanism, in which RNAs with miRNA response elements regulate each other, and exert their biological functions via means of sponging miRNAs (32,33). Our previous study confirmed the low expression of miR-455-3p in AML (34). Therefore, it was hypothesized that circPVT1 may be involved in the

ceRNA mechanism as a miR-455-3p sponge and serve a role in the progression of AML. miR-455-3p is an important tumor suppressor that serves an important role in numerous tumors, and reducing its expression can increase pancreatic cancer cell migration (35) and promote the malignant progression of colorectal cancer (36). By contrast, antagonism of miR-455-3p has been shown to inhibit chemoresistance and invasiveness in esophageal squamous cell carcinoma (37), and a similar effect has been observed in non-small cell lung cancer cells (38), triple-negative breast cancer cells (39) and A375 melanoma cells (40). Therefore, miR-455-3p may be closely related to human diseases; however, few studies (34) have investigated the potential regulatory mechanisms of miR-455-3p in AML. One aim of the current study was to identify the molecular mechanism of miR-455-3p in AML.

The present study explored the influence of MEF2A, a transcription factor of circPVT1, on the development of AML, and assessed the molecular mechanism underlying the involvement of miR-455-3p in the pathogenesis of AML.

## Materials and methods

*Collection of clinical data and patient samples.* Blood plasma samples from 42 patients with AML and 42 healthy controls (25 men and 17 women; mean age, 44.54 years; range, 19-76 years) were collected from The First Affiliated Hospital of Kunming Medical University (Kunming, China) between April 2021 and March 2022. The AML group consisted of 22 men and 20 women, with a mean age of 46.62 years (range, 16-80 years). The criteria for the selection of patients in this study included: i) Male or female patients with a body weight  $\geq 45$  kg; ii) no bleeding tendency; iii) no obvious abnormalities of heart, liver and kidney function; iv) expected survival,  $\geq 3$  months; v) women of childbearing age must have had a pregnancy test (serum or urine) within 7 days of enrollment, with a negative result, and be willing to use an appropriate method of contraception during the trial. Patients with other serious diseases or who started treatment within 3 months before admission were excluded, and those in the healthy control group had normal physiological function according to whole-body physiological examinations conducted at the aforementioned hospital. The diagnosis of AML was made according to the 2016 World Health Organization criteria (41). The basic information for all patients is shown in Table I. The present study was approved by the Ethics Committee of The First Affiliated Hospital of Kunming Medical University (approval no. L-10), and all individuals provided written informed consent for participation.

*Cell culture.* The following cell lines were used in the present study: A normal bone marrow stromal cell line (HS-5) and human AML cell lines (U937, THP-1, HL-60 and NB4), which were purchased from Shenzhen Haodi Huatuo Biotechnology Co., Ltd. All cells were cultured in DMEM (MilliporeSigma) containing 10% FBS (Gibco; Thermo Fisher Scientific, Inc.) and 1% penicillin/streptomycin (MilliporeSigma), and were incubated at 37°C in a 5% CO<sub>2</sub> incubator. The cells were subcultured when the cell density reached 90%. The cell lines used in the present study were authenticated by short tandem repeat profiling.

Table I. Clinical and biological characteristics of patients with AML.

Case	Age, years	Sex	WHO classification	Fusion gene	Mutation	Cytogenetics
1	40	Male	AML		FLT-ITD	Normal
2	58	Female	B-ALL			Normal
3	43	Female	AML		TP53	Normal
4	46	Female	AML	AML1-ETO		t(8;21)(q22;q22.1)
5	72	Female	AML			Normal
6	51	Female	AML		NPM1	Normal
7	25	Male	AML			Normal
8	66	Male	AML			Normal
9	51	Female	AML		RUNX1	Normal
10	51	Male	AML			Normal
11	77	Male	AML			Normal
12	23	Male	APL	PML-RARA		t(15;17)(q22;q12)
13	44	Female	AML	AML1-ETO		t(8;21)(q22;q22.1)
14	70	Female	AML			Normal
15	50	Male	AML		TP53	Normal
16	52	Female	AML			Normal
17	41	Male	AML			Normal
18	78	Male	APL		ASLX1	Normal
19	50	Female	APL	PML-RARA		t(15;17)(q22;q12)
20	47	Male	AML			Normal
21	23	Male	ALL	MLL-AF4		Normal
22	52	Female	ALL	BCR-ABL 210		t(9;22)(q34.1;q11.2)
23	45	Male	APL	PML-RARA	NPM1	t(15;17)(q22;q12)
24	48	Male	AML		ASLX1	Normal
25	57	Male	APL	PML-RARA		t(15;17)(q22;q12)
26	53	Male	AML			Normal
27	36	Male	APL	PML-RARA		t(15;17)(q22;q12)
28	50	Female	AML		NPM1	Normal
29	19	Male	AML			Normal
30	39	Male	B-ALL			Normal
31	35	Female	T-ALL			Normal
32	22	Female	AML			Normal
33	23	Male	T-ALL		NPM1	Normal
34	45	Female	AML			Normal
35	51	Female	AML			Normal
36	80	Female	AML			Normal
37	16	Male	AML			Normal
38	25	Male	AML			Normal
39	57	Female	AML	PML-RARA		t(15;17)(q22;q12)
40	49	Female	AML		TP53	Normal
41	34	Male	AML			Normal
42	64	Female	AML			Normal

ALL, acute lymphoblastic leukemia; APL, acute promyelocytic leukemia; B-ALL, acute B-lymphoblastic leukemia; T-ALL, acute T-lymphoblastic leukemia; WHO, World Health Organization.

CpG island region in the gene promoter of *circPVT1*. The *circPVT1* promoter region was identified by searching the UCSC database (<http://genome.ucsc.edu/>). Specifically, GRCh38/hg38 was used as the human reference genome. *CircPVT1* (hsa\_circ\_0085536) was located at chromosome

chr8:128806778-128903244, and the sequence 2,000 bp upstream of its transcription start site was selected as the promoter region. MethPrimer (<http://www.urogene.org/methprimer/>) (42) was used to analyze the CpG island regions in the *circPVT1* promoter sequence. Specifically,

the minimum CpG island length was set at 200 bp, the CpG percentage threshold was 50%, and the expected CpG island ratio threshold was 0.6.

*Gene promoter and transcription factor-binding sites of circPVT1.* The circPVT1 promoter sequence was identified as aforementioned. JASPAR (<https://jaspar.genereg.net/>) was used to analyze the transcription factors to which the circPVT1 promoter sequence might bind. The relative profile score threshold was set to 80%.

*Cell transfection.* NB4 or HL-60 cells were seeded at a density of  $2 \times 10^5$  cells/well, and were transfected with 50 nM miR-455-3p mimic, miR-455-3p inhibitor, small interfering RNA (siRNA/si)-PVT1, si-MCL1 and 2  $\mu$ g pcDNA3.1-MEF2A vector (oe-MEF2A) using Lipofectamine<sup>®</sup> 2000 (Invitrogen; Thermo Fisher Scientific, Inc.). Negative control (NC) mimic, NC inhibitor, NC-small interfering siRNA (NC-si) and pcDNA3.1 empty vector (NC-oe) were used as NCs. The cells were cultured at 37°C for 48 h. All oligonucleotides (Table SI) were designed and synthesized by Shanghai GenePharma Co., Ltd. The transfection efficiency was measured 48 h after transfection.

*Binding site query.* The biological information database StarBase (<http://starbase.sysu.edu.cn/>) was used to analyze the binding sites of circPVT1 and miR-455-3p or miR-455-3p and MCL1.

*Dual-luciferase reporter gene assay.* The circPVT1 and MCL1 3'UTRs containing the miR-455-3p binding site were cloned and inserted into the pGL3-Basic vector (Promega Corporation) to construct the PVT1-wild-type (WT) vector and the MCL1-WT vector, respectively. The 3'UTRs of circPVT1 and MCL1 containing mutant (MUT) binding sequences of miR-455-3p were also amplified and inserted into the pGL3-Basic vector downstream of the firefly luciferase gene to generate the PVT1-MUT vector and the MCL1-MUT vector. Subsequently, 293 T cells (Thermo Fisher Scientific, Inc.) were seeded in 24-well plates at a density of  $1.0 \times 10^5$ /ml per well. Subsequently, the WT or MUT vectors were cotransfected with the miR-455-3p mimic/inhibitor or NC mimic/inhibitor into 293T cells using Lipofectamine 2000. A total of 48 h after transfection, luciferase activity was measured using the dual-luciferase reporter gene assay system (Beyotime Institute of Biotechnology). In addition, pGL3-Basic-circPVT1 and pGL3-Basic-MEF2A vectors were transfected into NB4 cells using Lipofectamine 2000, followed by assessment using the aforementioned luciferase assay kit at 48 h post-transfection. Firefly luciferase activity was normalized to *Renilla* luciferase activity.

*Reverse transcription-quantitative PCR (RT-qPCR).* A TRIzol<sup>®</sup> RNA extraction kit (Invitrogen; Thermo Fisher Scientific, Inc.) was used to extract total RNA from AML cells or the blood plasma of patients with AML. First-strand cDNA was subsequently assembled using total RNA as a template with the PrimeScript RT Reagent kit (Takara Bio, Inc.) according to the manufacturer's protocol, and the cDNA obtained was used as a template for qPCR amplification. qPCR was performed

Table II. PCR primer sequences.

Gene	Sequence, 5'-3'
circPVT1	F: 5'-CCGACTCTTCCTGGTGAAGC-3' R: 5'-TGCTCGCAGCTCGTCG-3'
$\beta$ -actin	F: 5'-CATGTACGTTGCTATCCAGGC-3' R: 5'-CTCCTTAATGTCACGCACGAT-3'
miR-455-3p	F: 5'-CGGCAGTCCATGGGCAT-3' R: 5'-AGTGCAGGGTCCGAGGTATT-3'
U6	F: 5'-CTCGCTTCGGCAGCAC-3' R: 5'-AACGCTTCACGAATTTGCGT-3'
MCL1	F: 5'-CGCCAAGGACACAAAGCCAATG-3' R: 5'-AGCCAGCAGCACATTCCTGATG-3'
GAPDH	F: 5'-GGAGCGAGATCCCTCCAAAAT-3' R: 5'-GGCTGTTGTCATACTTCTCATGG-3'

F, forward; miR, microRNA; R, reverse.

according to the instructions of the SYBR Green qPCR kit (Thermo Fisher Scientific, Inc.), and the qPCR thermocycling conditions were 94°C for 2 min; followed by 45 cycles at 94°C for 15 sec and 60°C for 30 sec. GAPDH,  $\beta$ -actin and U6 were used as internal controls for circRNAs, mRNAs and miRNAs, respectively. Moreover, sterilized deionized water was used as a negative control for PCR in place of a nucleic acid template. The expression levels of genes were calculated using the  $2^{-\Delta\Delta Cq}$  method (43). The primer sequences are displayed in Table II.

*Agarose gel electrophoresis.* Agarose powder was dissolved in TBE buffer in a flask to prepare 2.5% agarose gel. After the agarose powder was completely dissolved, ethidium bromide was added and then poured into the gel-making plate. The PCR product of circPVT1 was then mixed with the loading buffer and applied to the gel, followed by electrophoresis; finally, the results were observed using a gel imaging system (Tanon Science & Technology Co., Ltd.).

*Argonaute 2-RNA immunoprecipitation (Ago2-RIP) assay.* NB4 cells were transfected with a NC mimic or inhibitor, and miR-455-3p mimic or inhibitor for 24 h, and a RIP experiment was performed using the Magna RIP RNA-Binding Protein Immunoprecipitation Kit (cat. no. 17-700; MilliporeSigma) according to previously described methods (44). RT-qPCR was performed as aforementioned to assess circPVT1 and MCL1 levels in Ago2 or IgG (negative control) immunoprecipitates.

*Stability verification.* RNase R (10 U/ $\mu$ l; Guangzhou Genesee Biotech. Co., Ltd.) was added to the experimental samples (2.5  $\mu$ g total RNA extracted from NB4 cells) at 37°C for 30 min. RT-qPCR was subsequently performed as aforementioned to verify the stability of circPVT1.

*Cell Counting Kit (CCK)-8 analysis of cell viability.* NB4 and HL-60 cell viability was assessed using a CCK-8 kit (Beyotime Institute of Biotechnology). The cells were added to 96-well plates at a concentration of  $3 \times 10^3$  cells/well and an equal amount

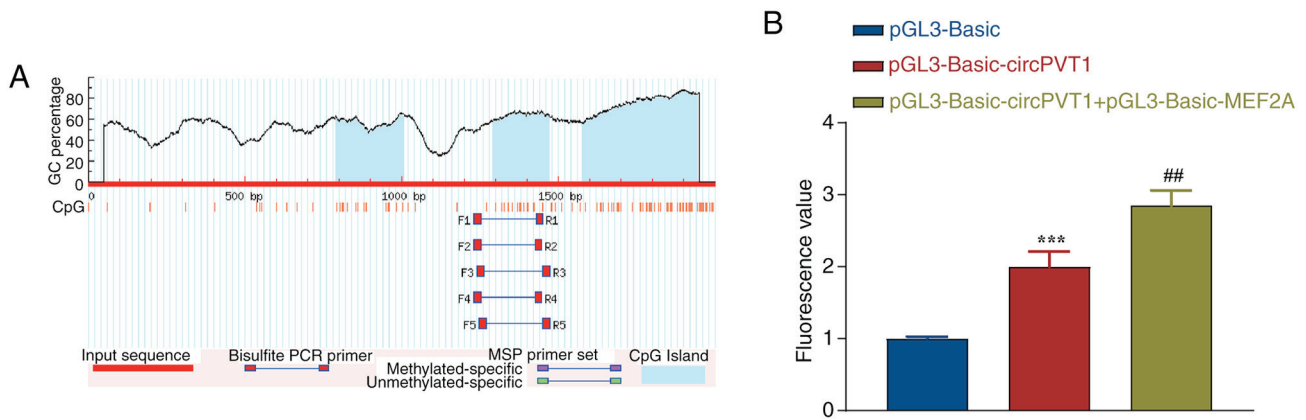


Figure 1. MEF2A acts as a transcription factor for circPVT1. (A) Prediction of the CpG islands in the promoter region of circPVT1. (B) MEF2A, a circPVT1 transcription factor, was analyzed by dual-luciferase assay. \*\*\* $P < 0.001$  vs. pGL3-Basic; ## $P < 0.01$  vs. pGL3-Basic-circPVT1. MEF2A, myocyte enhancer factor 2A.

of medium was added to each well. Subsequently, 10  $\mu$ l CCK-8 solution was added to each well and the plates were incubated at 37°C and 5% CO<sub>2</sub> for 2 h. The absorbance was measured at a wavelength of 450 nm using a microplate reader. As a blank control, CCK-8 solution was added to cell-free medium and the absorbance was measured at 450 nm.

**Detection of apoptosis by flow cytometry.** The cells from each group were collected and washed twice with precooled PBS. According to the manufacturer's protocol, the percentage of apoptotic cells was detected using an Annexin-V-FITC/PI apoptosis kit (Absin Bioscience, Inc.). Cells that were not stained with FITC or PI were used as negative controls. Cells were analyzed using a flow cytometer (FACSCalibur; BD Biosciences) and FlowJo-V10 software (FlowJo, LLC) was used to process the experimental results.

**Western blotting.** Total proteins were extracted from NB4 and HL-60 cells using RIPA lysis buffer (Beijing Solarbio Science & Technology Co., Ltd.), and the protein concentration was determined using a BCA kit (Beijing Solarbio Science & Technology Co., Ltd.). The proteins (40  $\mu$ g/lane) were subsequently separated by SDS-PAGE on 10% gels and were transferred to PVDF membranes. The membranes were blocked with 5% skim milk for 2 h at room temperature, and were then incubated with primary antibodies (Abcam) against MEF2A (1:1,000; cat. no. ab76063), caspase-3 (1:2,000; cat. no. ab184787), Bax (1:1,000; cat. no. ab32503), Bcl-2 (1:2,000; cat. no. ab182858), E-cadherin (1:1,000; cat. no. ab231303), N-cadherin (1:1,000; cat. no. ab245117), vimentin (1:1,000; cat. no. ab92547), fibronectin (1:1,000; cat. no. ab268020), and MCL1 (1:500; cat. no. ab243136) overnight at 4°C. GAPDH (1:1,000; cat. no. ab181602) was used as the internal reference protein. The membrane was subsequently incubated with an HRP-conjugated secondary antibody (1:2,000; cat. no. ab288151; Abcam) for 1 h at room temperature. The protein bands were visualized with an enhanced chemiluminescence detection kit (BD Biosciences), and ImageJ 1.8.0.345 software (National Institutes of Health) was used for protein band gray value analysis. In addition, nuclear and cytoplasmic proteins were isolated from NB4 and HL-60 cells using a Nuclear and Cytoplasmic Protein Extraction Kit (Beyotime Institute

of Biotechnology) according to the manufacturer's instructions. H3 (1:1,000; cat. no. ab1791; Abcam) was used as the internal reference for nuclear proteins and western blotting was performed as aforementioned.

**Statistical analysis.** The cell experiments were repeated three times. All experimental data are presented as the mean  $\pm$  standard deviation. GraphPad Prism 7 (Dotmatics) was used to analyze and plot the data. For normally distributed and homogeneous variance variables, unpaired Student's t-test was used for comparisons between two groups, and one-way ANOVA was used for comparisons between multiple groups, followed by Tukey's multiple comparisons test. The Mann-Whitney U test was used for nonparametric data. The correlations between circPVT1 and miR-455-3p, miR-455-3p and MCL1, or circPVT1 and MCL1 were assessed by Pearson correlation analysis.  $P < 0.05$  was considered to indicate a statistically significant difference.

## Results

**MEF2A is a transcription factor for circPVT1.** To explore the role of MEF2A as a transcription factor of circPVT1 in the malignant development of AML, the promoter region of circPVT1 was first analyzed. As shown in Fig. 1A, the promoter region of circPVT1 was enriched in CpG islands, forming an obvious CG enrichment phenomenon, and three CpG islands were identified via Meth Primer analysis. The sizes of CpG islands 1, 2 and 3 were 217, 183 and 368 bp, respectively. CpG islands often appear in the promoter region and can affect the affinity of the promoter for transcription factors. The binding sites of the circPVT1 promoter were then analyzed, and it was revealed that 34 sequences could bind to the circPVT1 promoter (Table III). It was revealed that the transcription factor MEF2A can bind to the circPVT1 promoter region with high affinity. Subsequently, the pGL3-Basic-circPVT1 and pGL3-Basic-MEF2A eukaryotic expression vectors were cotransfected into NB4 cells. The empty vector pGL3-Basic was used as a control, and the luciferase activity was detected after transfection for 24 h. Compared with the pGL3-Basic-circPVT1 group, the cells cotransfected with pGL3-Basic-circPVT1 and pGL3-Basic-MEF2A group

Table III. Prediction results of transcription factor binding sites.

Matrix ID	Name	Score	Relative score	Sequence ID	Start	End	Strand	Predicted sequence
MA0693.2	MA0693.2.VDR	11.801543	0.999999973578093	NC_000008.11:128902835-128904835	317	324	+	TGAGTTCA
MA0909.3	MA0909.3.Hoxd13	14.179089	0.9940158898993562	NC_000008.11:128902835-128904835	1,749	1,758	-	GGCAATAAA
MA0909.3	MA0909.3.Hoxd13	14.126415	0.9930206731735303	NC_000008.11:128902835-128904835	1,640	1,649	+	AACAATAAA
MA0136.1	MA0136.1.ELF5	11.374968	0.992970134254861	NC_000008.11:128902835-128904835	1,147	1,155	-	TATTTCCCT
MA0693.3	MA0693.3.Vdr	13.322502	0.990863401631873	NC_000008.11:128902835-128904835	316	326	+	CTGAGTTCAAA
MA0909.1	MA0909.1.HOXD13	14.127036	0.9777348702657696	NC_000008.11:128902835-128904835	1,748	1,757	-	GCAATAAAA
MA0769.2	MA0769.2.TCF7	13.55147	0.9764263544920703	NC_000008.11:128902835-128904835	1,708	1,718	+	TTCTTTGAAAGT
MA0769.2	MA0769.2.TCF7	12.878226	0.9621331874851317	NC_000008.11:128902835-128904835	1,389	1,399	+	ATCTTTGAACT
MA0909.2	MA0909.2.HOXD13	14.661904	0.9550868989404843	NC_000008.11:128902835-128904835	1,748	1,758	-	GGCAATAAAA
MA0136.3	MA0136.3.Elf5	13.925515	0.9502244196272698	NC_000008.11:128902835-128904835	169	180	+	AGAAGGAAGGAA
MA0909.3	MA0909.3.Hoxd13	11.67624	0.9467267523321995	NC_000008.11:128902835-128904835	1,961	1,970	+	GCCAATAACA
MA0693.2	MA0693.2.VDR	9.756103	0.9416772888554328	NC_000008.11:128902835-128904835	1,608	1,615	+	TGAGTTTA
MA0505.2	MA0505.2.Nr5A2	15.631966	0.9398028693468796	NC_000008.11:128902835-128904835	1,845	1,857	+	TTGACCTTGAGCA
MA0136.3	MA0136.3.Elf5	13.174745	0.9358547814540202	NC_000008.11:128902835-128904835	173	184	+	GGAAGGAAGGGA
MA0602.1	MA0602.1.Arid5a	12.836242	0.9334683286303311	NC_000008.11:128902835-128904835	682	695	+	TAAATATTAAAT
MA0507.1	MA0507.1.POU2F2	14.1472435	0.9318346396422754	NC_000008.11:128902835-128904835	1,989	2,001	+	TGATTTTGCATGT
MA0136.3	MA0136.3.Elf5	12.702013	0.9268067684029953	NC_000008.11:128902835-128904835	212	223	+	TGAAGGAAGGAA
MA0602.1	MA0602.1.Arid5a	12.536406	0.9263717295874732	NC_000008.11:128902835-128904835	233	246	+	TAAATATTGTTAAC
MA0602.1	MA0602.1.Arid5a	12.319698	0.9212426473424906	NC_000008.11:128902835-128904835	915	928	-	TCAATATTCTATT
MA0602.1	MA0602.1.Arid5a	12.213568	0.9187307211047131	NC_000008.11:128902835-128904835	919	932	+	GAAATATTGAGACT
MA0660.1	MA0660.1.MEF2B	13.488233	0.9172942646213134	NC_000008.11:128902835-128904835	1,928	1,939	+	ACTACAATAGC
MA0052.4	MA0052.4.MEF2A	14.876074	0.9166135549477946	NC_000008.11:128902835-128904835	908	922	+	GGCAAAAATAGAAA
MA0773.1	MA0773.1.MEF2D	12.476424	0.9156625804509553	NC_000008.11:128902835-128904835	1,928	1,939	+	ACTACAATAGC
MA0136.1	MA0136.1.ELF5	8.871671	0.9111586439845092	NC_000008.11:128902835-128904835	171	179	-	TCCTTCCTT
MA0136.1	MA0136.1.ELF5	8.871671	0.9111586439845092	NC_000008.11:128902835-128904835	214	222	-	TCCTTCCTT
MA0136.1	MA0136.1.ELF5	8.865436	0.9109548708370724	NC_000008.11:128902835-128904835	1,116	1,124	-	CAGTTCCTT
MA0052.1	MA0052.1.MEF2A	12.713359	0.9095717752732639	NC_000008.11:128902835-128904835	1,929	1,938	-	CTATTTGTAG
MA0773.1	MA0773.1.MEF2D	11.798319	0.9081350993833815	NC_000008.11:128902835-128904835	909	920	+	GCAAAAATAGA
MA0052.2	MA0052.2.MEF2A	13.31947	0.9071642295567492	NC_000008.11:128902835-128904835	1,099	1,113	-	CACCAAAAATAACAC
MA0136.1	MA0136.1.ELF5	8.708229	0.9058171258167399	NC_000008.11:128902835-128904835	960	968	-	AATTCCTA
MA0052.3	MA0052.3.MEF2A	12.794866	0.9046434712727364	NC_000008.11:128902835-128904835	909	920	+	GCAAAAATAGA
MA0769.2	MA0769.2.TCF7	10.165019	0.9045309633699953	NC_000008.11:128902835-128904835	1,129	1,139	-	AGCTTTGATTG
MA0136.1	MA0136.1.ELF5	8.656569	0.9041287820729873	NC_000008.11:128902835-128904835	218	226	-	TCCTTCCTT
MA0909.1	MA0909.1.HOXD13	10.085875	0.9031867671283802	NC_000008.11:128902835-128904835	1,641	1,650	+	ACAATAAAG

showed a significant increase in luciferase activity (Fig. 1B). These results indicated that the MEF2A gene can significantly increase circPVT1 promoter activity.

**Abnormal expression of circPVT1 in AML.** Evaluation by RT-qPCR revealed that the expression levels of circPVT1 were markedly elevated in the AML group compared with those in the healthy control group (Fig. 2A). These findings suggested that circPVT1 may be highly expressed in the blood plasma of patients with AML. Moreover, the expression levels of circPVT1 were evaluated in different AML cell lines and it was demonstrated that circPVT1 expression was greater in AML cell lines (U937, THP-1, HL-60 and NB4) compared with that in HS-5 cells; this effect was particularly pronounced in NB4 and HL-60 cells (Fig. 2B). Therefore, NB4 and HL-60 cells were selected for subsequent experiments. In addition, data analysis on circPVT1 we performed using the UCSC Genome Browser and it was revealed that circPVT1 was circularized from the PVT1 gene and located on chr8:128806778-128903244 (Fig. 2C). The length of the spliced mature sequence of circPVT1 was 777 bp according to agarose gel electrophoresis (Fig. 2D). Finally, RNase R, a 3' exonuclease that has no effect on circRNAs (45), was added to the experimental samples to verify the stability of circPVT1. The RT-qPCR results revealed that RNase R had no significant effect on the expression levels of circPVT1. However, linear PVT1 was digested by RNase R (Fig. 2E). These results demonstrated that circPVT1 has greater stability.

**MEF2A affects the viability and apoptosis of AML cells via circPVT1.** To investigate the effect of MEF2A on AML cells, NB4 and HL-60 cells were transfected with the MEF2A overexpression vector (oe-MEF2A), with NC-oe as the control. The results of western blotting revealed that the expression levels of MEF2A showed a clear upward trend in cells post-transfection with oe-MEF2A, indicating successful overexpression of MEF2A (Fig. 3A). After successful transfection, the results of RT-qPCR revealed that, compared with in the NC group, the overexpression of MEF2A promoted the expression of circPVT1 in the cells (Fig. 3B). Furthermore, the results of the CCK-8 assay revealed that overexpression of MEF2A significantly increased the viability of NB4 and HL-60 cells (Fig. 3C). Next, the apoptosis of NB4 and HL-60 cells after oe-MEF2A transfection was detected by flow cytometry. Compared with that in the NC group, apoptosis was significantly inhibited after MEF2A overexpression (Fig. 3D). Moreover, western blotting was used to detect the expression of apoptosis-related proteins, and MEF2A overexpression inhibited the expression of the proapoptotic proteins caspase-3 and Bax, and promoted the expression levels of the antiapoptotic protein Bcl-2 in AML cells (Fig. 3E), which was consistent with the results of flow cytometry. In summary, MEF2A overexpression markedly inhibited the apoptosis of AML cells. In addition, EMT serves a key role in tumor progression by allowing cells to metastasize and invade (46). Western blotting was used to detect the expression levels of EMT marker proteins. It was revealed that the expression levels of the epithelial marker E-cadherin were downregulated, whereas the expression levels of the mesenchymal markers N-cadherin, vimentin and fibronectin were upregulated after MEF2A was

overexpressed in NB4 and HL-60 cell lines, indicating that MEF2A overexpression promoted the EMT process in NB4 and HL-60 cells (Fig. 3F). Taken together, these findings suggested that MEF2A may promote the malignant progression of AML cells through circPVT1.

**CircPVT1 targets and regulates miR-455-3p expression.** To explore the role of circPVT1 in AML, the biological information database StarBase was used to analyze circPVT1 target genes, and it was revealed that circPVT1 could bind to miR-455-3p (Fig. 4A). RT-qPCR was used to detect the transfection efficiency of the miR-455-3p mimic. The results showed that transfection with the miR-455-3p mimic significantly increased the expression levels of miR-455-3p in cells compared with those in the NC mimic group, indicating successful transfection (Fig. 4B). Moreover, a dual-luciferase reporter gene assay was used to verify the relationship between circPVT1 and miR-455-3p. The results revealed that the miR-455-3p mimic or the miR-455-3p inhibitor significantly affected the luciferase activity of the PVT1-WT vector, whereas there was no significant effect on the luciferase activity of the PVT1-MUT vector (Fig. 4C). Ago2-RIP assay was further used to verify the binding relationship between circPVT1 and miR-455-3p, and the IgG group was used as a negative control. The results revealed that circPVT1 was enriched by the miR-455-3p mimic, whereas the miR-455-3p inhibitor did not enrich circPVT1 (Fig. 4D). These results indicated that circPVT1 may have a targeted binding relationship with miR-455-3p. In addition, after evaluation by RT-qPCR, it was revealed that the expression levels of miR-455-3p showed a clear downward trend in the AML group compared with those in the healthy control group (Fig. 4E). Pearson correlation analysis revealed that miR-455-3p and circPVT1 were negatively correlated; however, the R-value was <0.3, indicating that the relationship was weak (Fig. 4F). Thus, these results identified an interaction between miR-455-3p and circPVT1, and indicated that circPVT1 may negatively regulate miR-455-3p.

**CircPVT1 promotes the viability and EMT of AML cells through miR-455-3p.** The present study next explored how circPVT1 affects the viability and EMT of AML cells through miR-455-3p. Cells were transfected with the miR-455-3p inhibitor and/or si-circPVT1, and the transfection efficiency was detected by RT-qPCR. The results revealed that transfection with the miR-455-3p inhibitor significantly decreased the expression levels of miR-455-3p in cells, and knockdown of circPVT1 significantly reduced circPVT1 expression levels compared with those in the NC inhibitor or NC-si groups, thus indicating successful transfection (Fig. 5A). The NC group in Fig. 5B-E refers to NB4 and HL-60 cells without any treatment. Next, cell viability was detected by a CCK-8 assay. The results revealed that circPVT1 knockdown significantly inhibited the viability of NB4 and HL-60 cells, whereas miR-455-3p inhibitor transfection weakened the effect of circPVT1 knockdown and promoted cell viability (Fig. 5B). Moreover, flow cytometry revealed that si-circPVT1 promoted apoptosis, whereas the miR-455-3p inhibitor weakened the effect of si-circPVT1 and inhibited apoptosis (Fig. 5C). Western blot analysis of apoptosis-related proteins

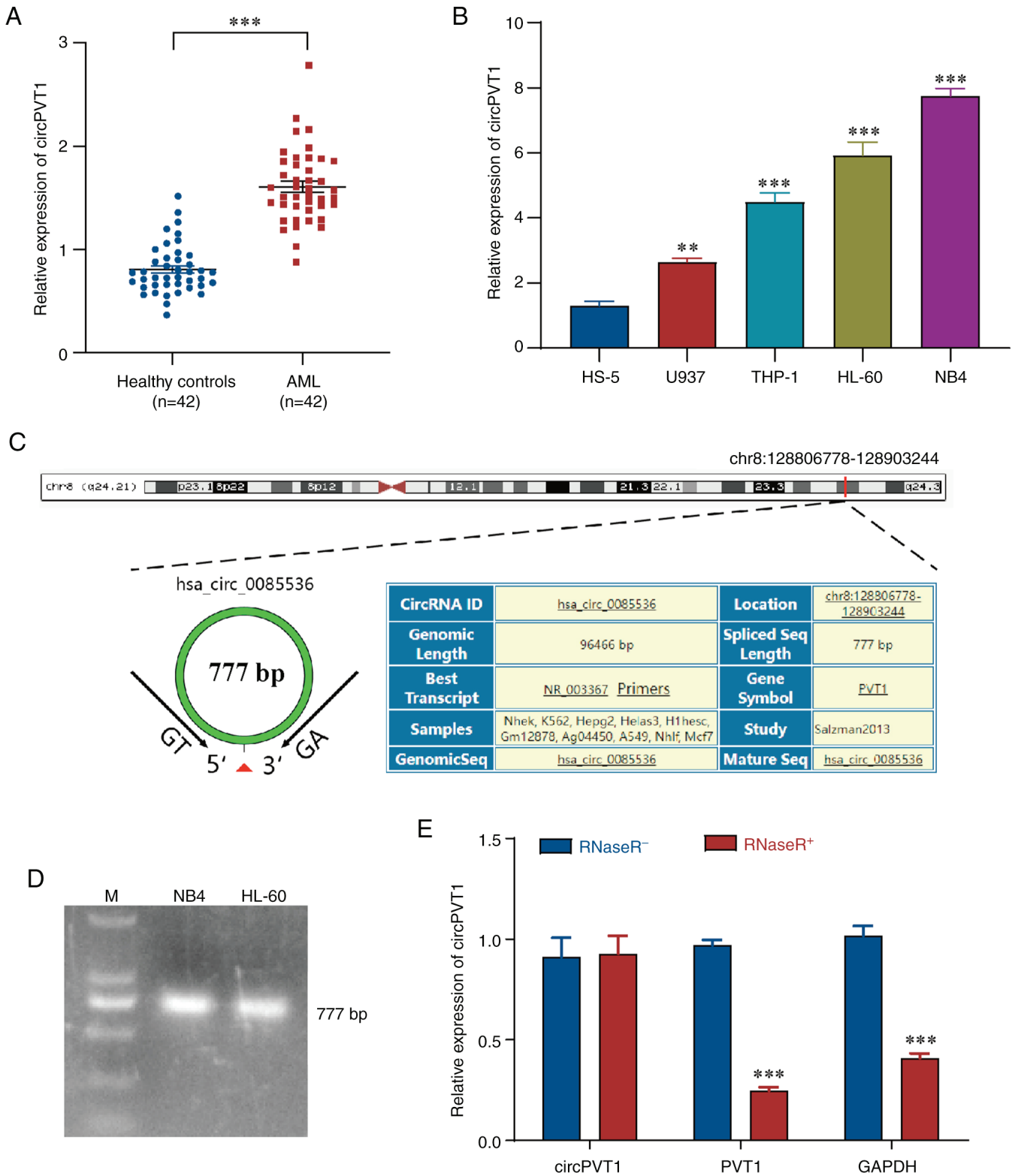


Figure 2. Aberrant expression of circPVT1 in AML. (A) RT-qPCR analysis of the expression levels of circPVT1 in plasma samples from patients with AML. \*\*\* $P < 0.001$ . (B) RT-qPCR analysis of the expression levels of circPVT1 in AML cell lines and HS-5 cells. \*\* $P < 0.01$ , \*\*\* $P < 0.001$  vs. HS-5 cells. (C) Mature sequence length of circPVT1 was analyzed via the UCSC database. (D) Mature sequence of circPVT1 splicing was detected by agarose gel electrophoresis. (E) Effect of RNase R on the expression of circPVT1 was detected via RT-qPCR. \*\*\* $P < 0.001$  vs. RNase R<sup>-</sup>. AML, acute myeloid leukemia; RT-qPCR, reverse transcription-quantitative PCR.

in NB4 and HL-60 cells revealed that cotransfection with si-circPVT1 and the miR-455-3p inhibitor reversed the promoting effect of si-PVT1 on caspase-3 and Bax, and its inhibitory effect on Bcl-2 (Fig. 5D). In addition, the expression

of EMT-related proteins was detected by western blotting, and it was demonstrated that the expression levels of E-cadherin were increased, whereas those of N-cadherin, vimentin and fibronectin were decreased after circPVT1 was knocked down.



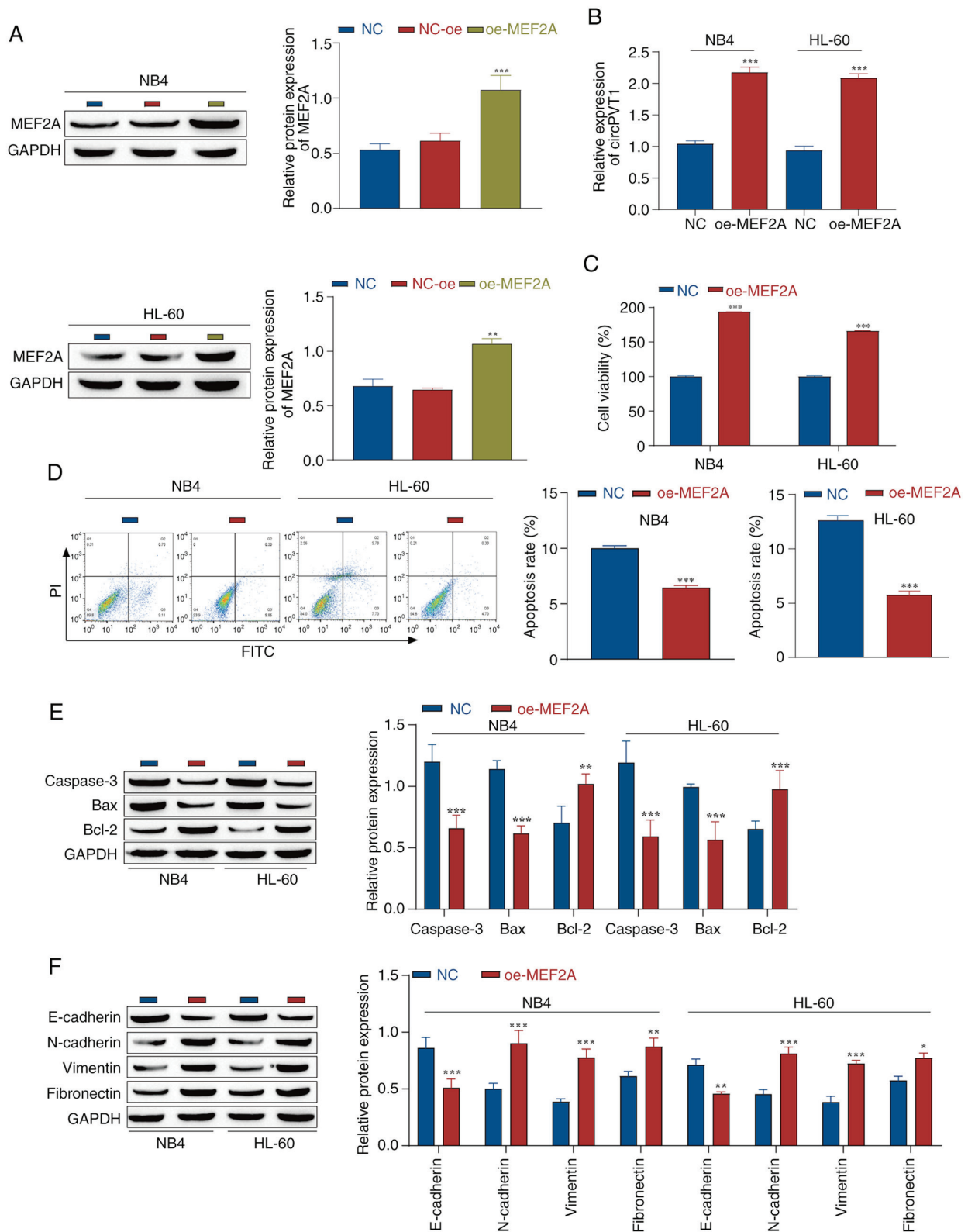


Figure 3. Effect of MEF2A, a transcription factor for circPVT1, on the viability and apoptosis of acute myeloid leukemia cells. (A) Western blot analysis of the transfection efficiency of oe-MEF2A in NB4 and HL-60 cells. \*\* $P < 0.01$ , \*\*\* $P < 0.001$  vs. NC-oe. (B) Reverse transcription-quantitative PCR analysis of the levels of circPVT1. (C) Cell Counting Kit-8 analysis of viability. (D) Flow cytometric analysis of apoptosis. (E) Western blot analysis of the expression levels of apoptosis-related proteins. (F) Western blot analysis of the expression levels of epithelial-mesenchymal transition-related proteins. \* $P < 0.05$ , \*\* $P < 0.01$ , \*\*\* $P < 0.001$  vs. NC. MEF2A, myocyte enhancer factor 2A; NC, negative control; oe, overexpression.

However, after transfection with the miR-455-3p inhibitor, the opposite results were observed and the effects of si-circPVT1 were markedly reversed (Fig. 5E). These data suggested that

circPVT1 knockdown may promote apoptosis and inhibit the progression of EMT, whereas miR-455-3p knockdown could alleviate the effects of circPVT1 knockdown, thereby

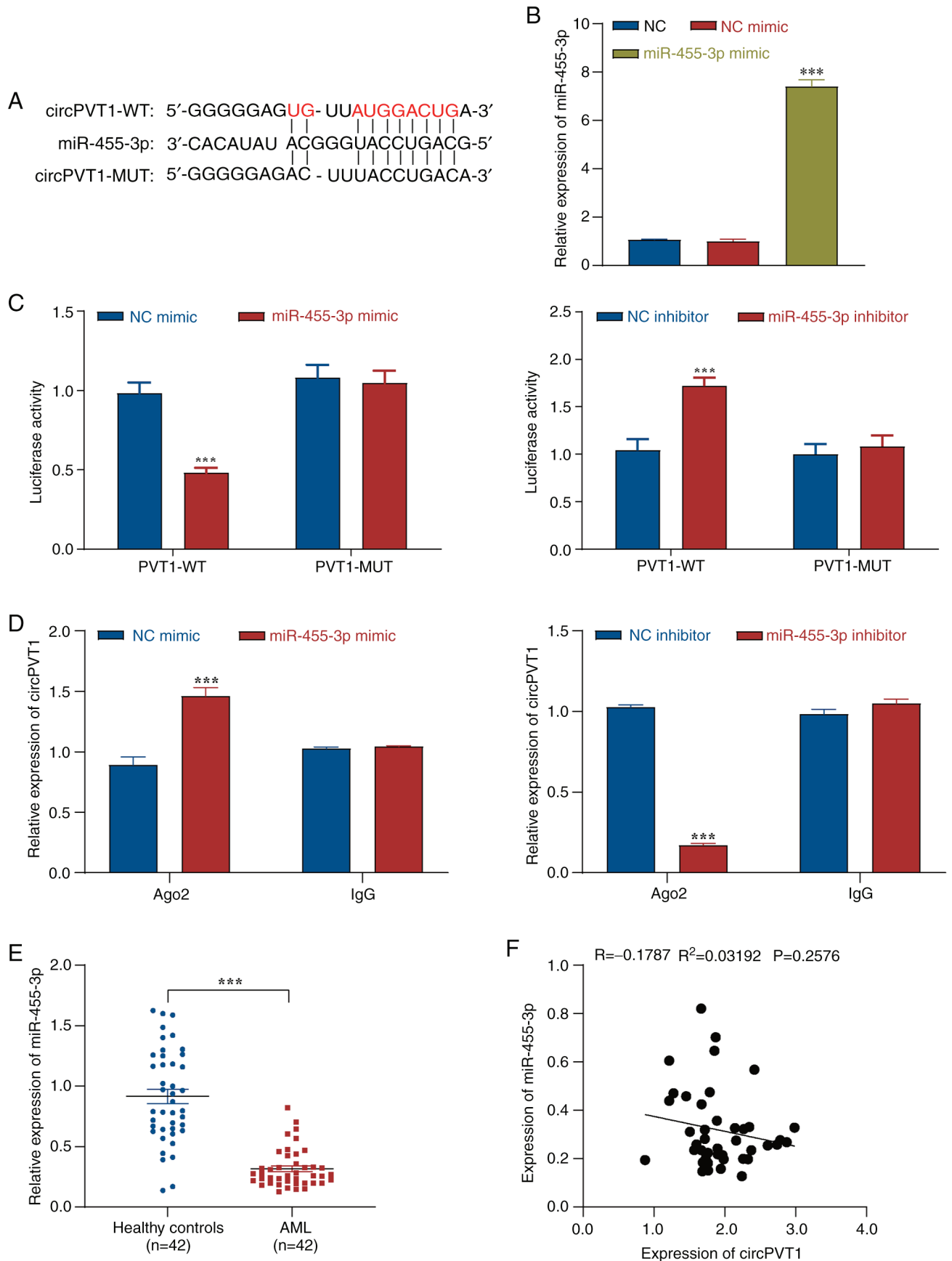


Figure 4. CircPVT1 targets and regulates miR-455-3p expression. (A) miR-455-3p binding sequence to circPVT1. (B) Transfection efficiency of the miR-455-3p mimic was detected by RT-qPCR. (C) Dual-luciferase gene reporter assay verified the targeting relationship between miR-455-3p and circPVT1. (D) Ago2-RNA immunoprecipitation assay was used to detect the relationship between miR-455-3p and circPVT1. (E) RT-qPCR analysis the expression levels of miR-455-3p in plasma samples from patients with AML. (F) Correlation analysis of miR-455-3p and circPVT1. \*\*\* $P<0.001$  vs. NC mimic or as indicated. Ago2, argonaute 2; AML, acute myeloid leukemia; miR, microRNA; MUT, mutant; NC, negative control; RT-qPCR, reverse transcription-quantitative PCR; WT, wild-type.

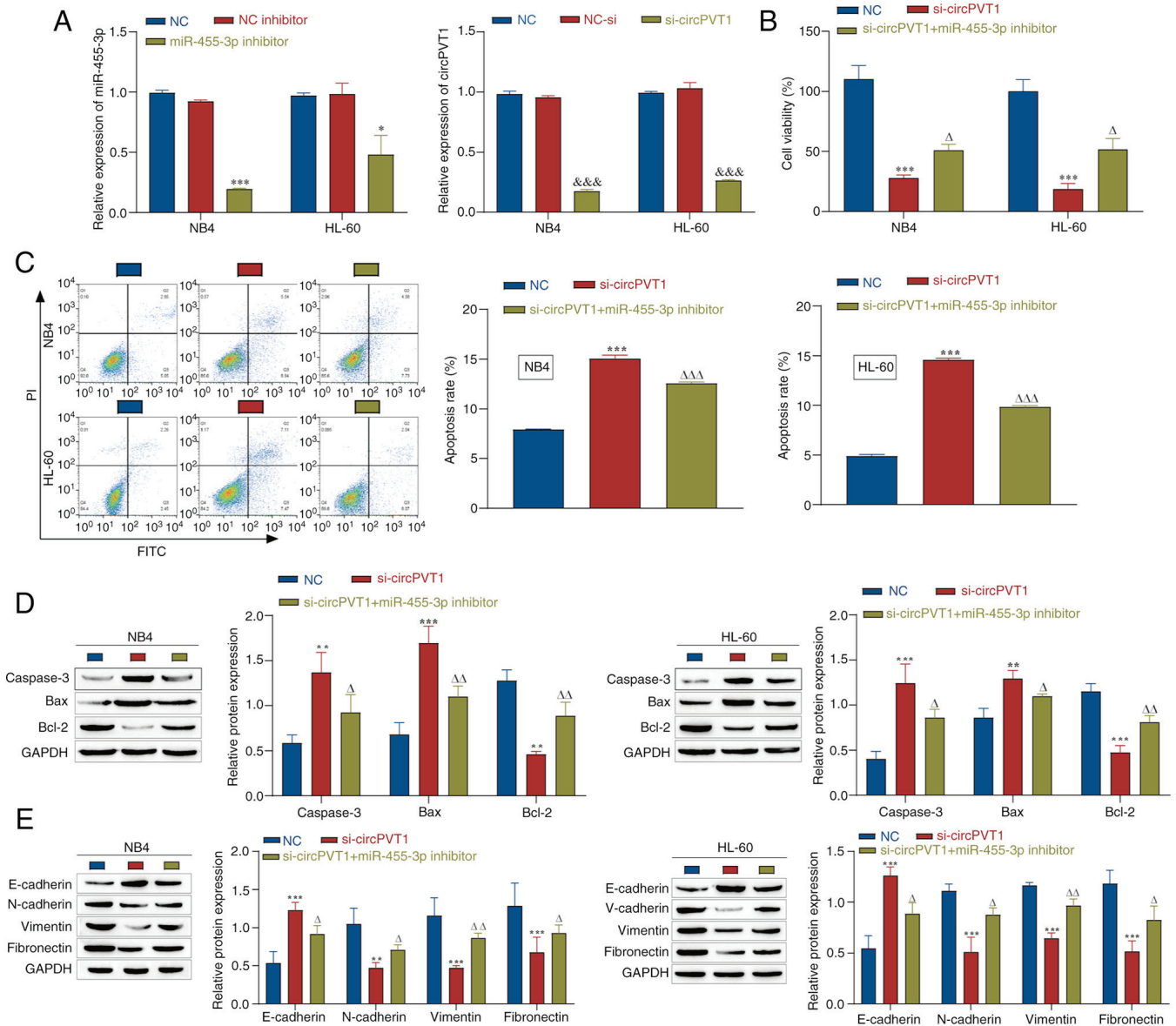


Figure 5. CircPVT1 promotes the viability and EMT of NB4 and HL-60 cells through miR-455-3p. (A) Transfection efficiency of the miR-455-3p inhibitor or si-PVT1 was detected by reverse transcription-quantitative PCR. \* $P < 0.05$ , \*\*\* $P < 0.001$  vs. NC inhibitor; &&& $P < 0.001$  vs. NC-si. (B) Cell Counting Kit-8 was used to detect viability. (C) Apoptosis was detected by flow cytometry. (D) Western blotting was used to detect the expression levels of apoptosis-related proteins. (E) Western blotting was used to detect the expression levels of EMT-related proteins, \*\* $P < 0.01$ , \*\*\* $P < 0.001$  vs. NC;  $\Delta P < 0.05$ ,  $\Delta\Delta P < 0.01$ ,  $\Delta\Delta\Delta P < 0.001$  vs. si-circPVT1 group. EMT, epithelial-mesenchymal transition; miR, microRNA; NC, negative control; si, small interfering.

inhibiting apoptosis and promoting the progression of EMT. In summary, miR-455-3p is associated with the regulatory effects of circPVT1 on AML cell viability and EMT.

*miR-455-3p targets and regulates MCL1 expression.* MCL1 has been shown to be upregulated in patients with AML, and it has been suggested that MCL1 is associated with poor prognosis in patients with AML and could be used for disease surveillance (47). In addition, Lu *et al* (48) revealed that miR-181b could improve the drug resistance of AML cells by decreasing the levels of MCL1. Therefore, it was hypothesized that MCL1 may be a target of miR-455-3p, and that miR-455-3p may regulate the progression of AML by targeting MCL1. First, the expression of MCL1 in the nucleus and cytoplasm of NB4 and HL-60 cells was detected by western blotting. The results indicated that MCL1 was mainly

expressed in the nucleus (Fig. 6A). StarBase predicted that MCL1 would be targeted by miR-455-3p (Fig. 6B). Moreover, dual-luciferase reporter gene and Ago2-RIP assays were used to verify the targeting relationship between miR-455-3p and MCL1. The results of the dual-luciferase reporter gene assay revealed that the miR-455-3p mimic reduced the luciferase activity of the MCL1-WT vector but had no significant effect on the luciferase activity of the MCL1-MUT vector (Fig. 6C). The Ago2-RIP assay results revealed that the miR-455-3p mimic significantly enriched MCL1; the IgG group was used as a negative control (Fig. 6D). These results indicated that miR-455-3p may interact with MCL1. In addition, after evaluation by RT-qPCR, the results revealed that the expression levels of MCL1 exhibited a clear upward trend in the plasma of patients with AML compared with in those from healthy controls (Fig. 6E). The relationship between miR-455-3p

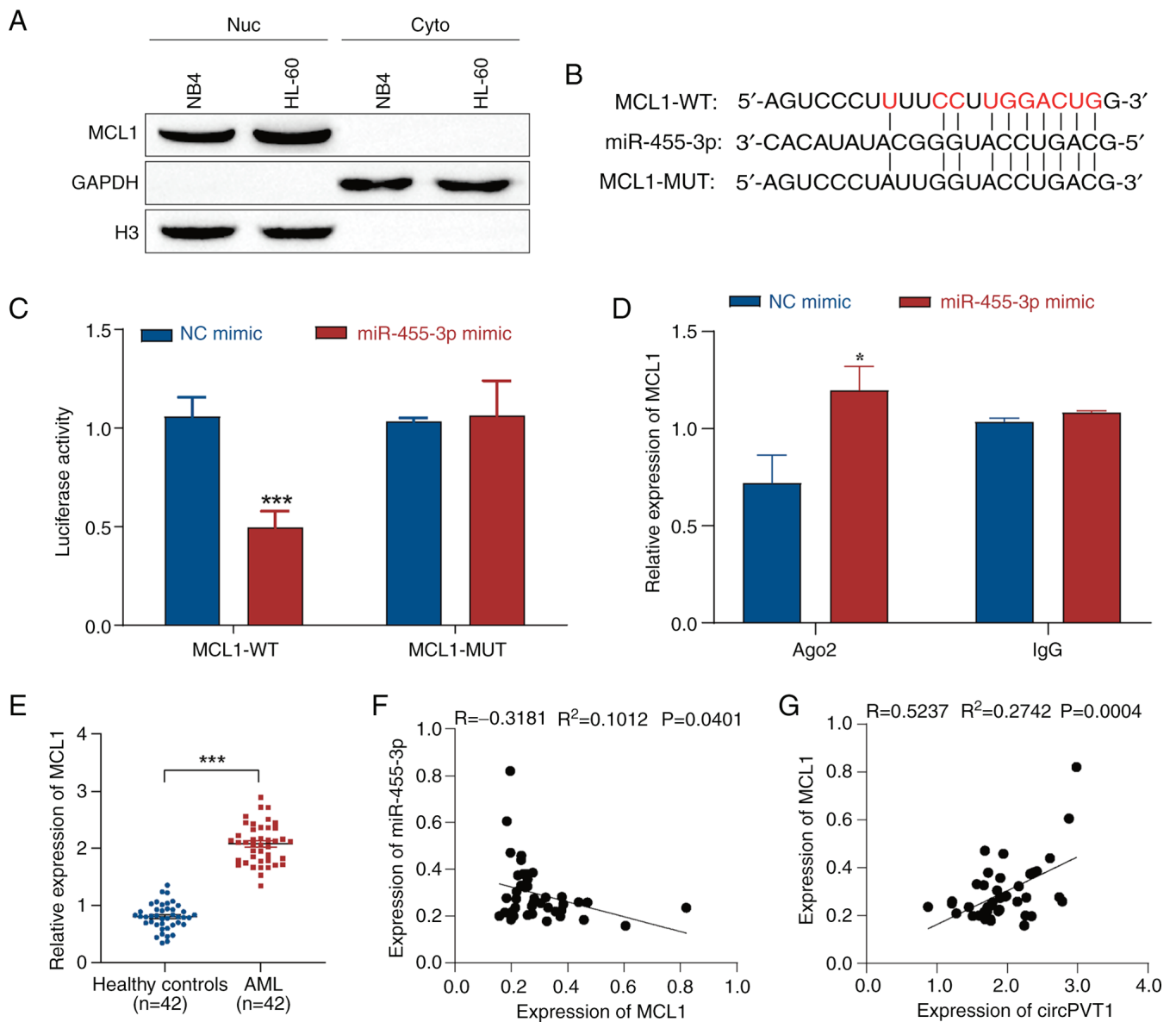


Figure 6. miR-455-3p regulates MCL1 expression. (A) Expression of MCL1 in the nucleus and cytoplasm of NB4 and HL-60 cells was detected by western blotting. (B) MCL1 binding sequence to miR-455-3p. (C) Dual-luciferase reporter gene assay verified the targeting relationship between miR-455-3p and MCL1. (D) Ago2-RNA immunoprecipitation assay. (E) Reverse transcription-quantitative PCR was used to measure the expression levels of MCL1 in the plasma of patients with AML. (F) Correlation analysis of miR-455-3p and MCL1. (G) Correlation analysis of MCL1 and circPVT1. \* $P < 0.05$ , \*\*\* $P < 0.001$  vs. NC mimic or as indicated. Ago2, argonaute 2; AML, acute myeloid leukemia; miR, microRNA; MUT, mutant; NC, negative control; WT, wild-type.

and MCL1 was then analyzed by correlation analysis, which revealed that miR-455-3p was negatively correlated with MCL1 (Fig. 6F). In addition, MCL1 was positively correlated with circPVT1 (Fig. 6G). These results suggested that MCL1 may be a target gene of miR-455-3p and could serve an important role in circPVT1/miR-455-3p-mediated AML.

*CircPVT1 promotes the viability and EMT of AML cells through the miR-455-3p/MCL1 axis.* The present study further explored how circPVT1 influences the malignant progression of AML through the miR-455-3p/MCL1 axis. Following the observation that knockdown of circPVT1 and miR-455-3p affected the viability and EMT of NB4 and HL-60 cells, the effects of MCL1 knockdown on these cells were further explored. First, si-MCL1 was transfected into the cells, and the transfection efficiency was detected by western blotting.

The expression levels of MCL1 in the si-MCL1 group were significantly lower than those in the NC-si group, indicating successful transfection (Fig. 7A and B). The NC group in Fig. 7C-F refers to NB4 and HL-60 cells without any treatment. The CCK-8 assay was used to assess the effects on cell viability, and it was revealed that knockdown of MCL1 weakened the effect of the miR-455-3p inhibitor, and inhibited the viability of NB4 and HL-60 cells (Fig. 7C). Moreover, flow cytometry was used to detect apoptosis, and the results showed that the knockdown of MCL1 promoted apoptosis compared with that in the si-circPVT1 + miR-455-3p inhibitor group (Fig. 7D). Furthermore, western blotting was used to detect the expression levels of apoptosis-related proteins. Notably, si-MCL1 partially reversed the effect of the miR-455-3p inhibitor, and promoted the expression of Caspase-3 and Bax, and inhibited the expression of Bcl-2 (Fig. 7E). In addition,

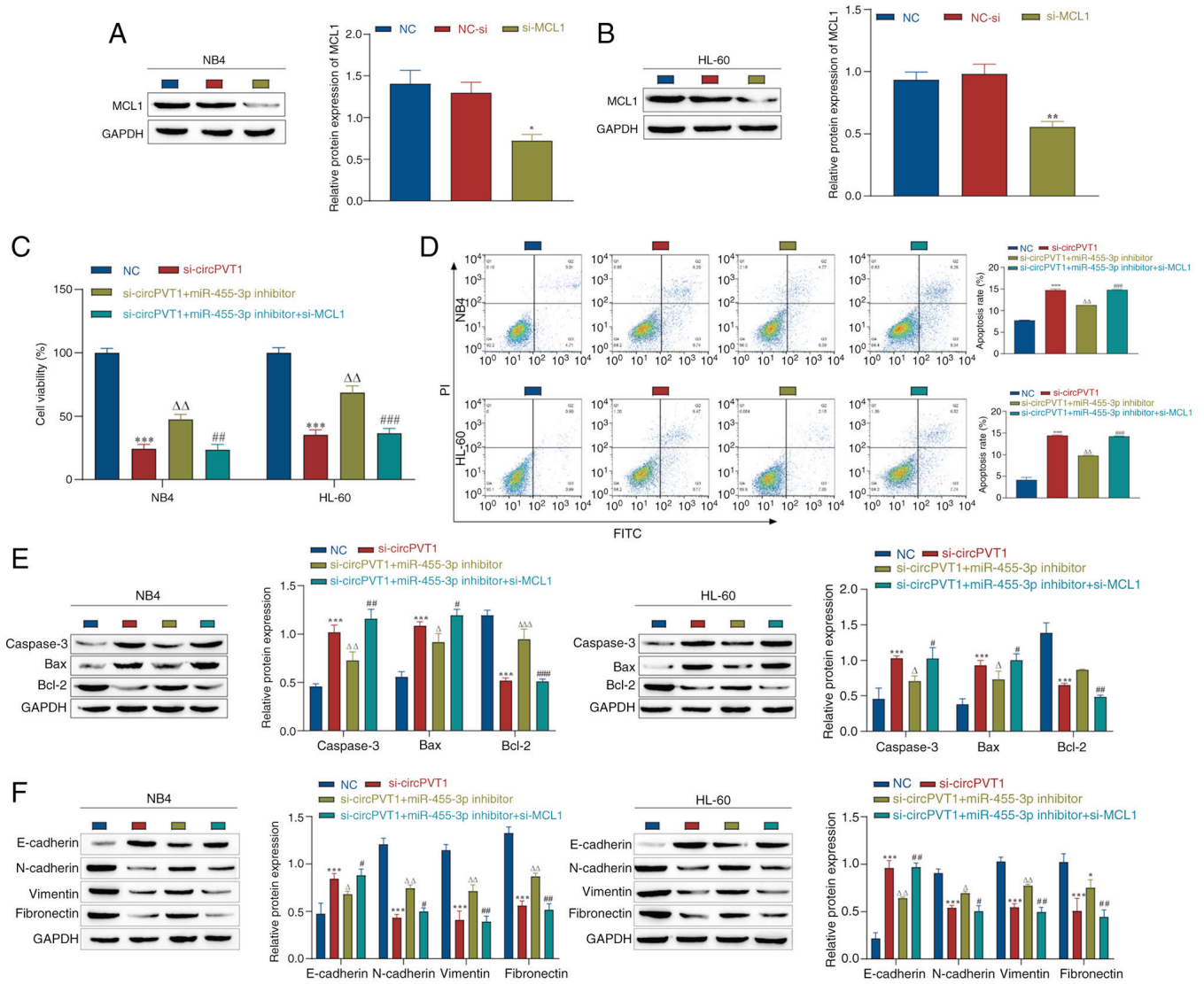


Figure 7. circPVT1 knockdown mediates the malignant growth of acute myeloid leukemia cells by regulating miR-455-3p/MCL1. Western blot analysis post-transfection with si-MCL1 in (A) NB4 and (B) HL-60 cells. \* $P < 0.05$ , \*\* $P < 0.01$  vs. NC-si. (C) Cell Counting Kit-8 assay of proliferation. (D) Flow cytometric analysis of apoptosis; (E) Western blot analysis of the expression levels of apoptosis-related proteins. (F) Western blot analysis of the expression levels of epithelial-mesenchymal transition-related proteins. \*\*\* $P < 0.001$  vs. NC;  $\Delta P < 0.05$ ,  $\Delta\Delta P < 0.01$ ,  $\Delta\Delta\Delta P < 0.001$  vs. si-circPVT1;  $\# P < 0.05$ ,  $\#\# P < 0.01$ ,  $\#\#\# P < 0.001$  vs. si-circPVT1 + miR-455-3p inhibitor. miR, microRNA; NC, negative control; si, small interfering.

the expression levels of EMT-related markers were detected by western blotting. The results showed that si-MCL1 promoted the expression levels of E-cadherin, and inhibited the expression levels of N-cadherin, vimentin and fibronectin compared with those in the si-circPVT1 + miR-455-3p inhibitor group (Fig. 7F). These data indicated that further knockdown of MCL1 may weaken the effects of the miR-455-3p inhibitor, promote the apoptosis of AML cells, and inhibit cell viability and the EMT process. These findings suggested that circPVT1 could influence the malignant progression of AML through the miR-455-3p/MCL1 axis.

### Discussion

Despite the current advances in the treatment of AML, including immunotherapy, its treatment remains challenging due to drug resistance and relapse (49). Therefore, fully understanding the molecular mechanism of AML occurrence

and development, and exploring new molecular therapeutic strategies are important. In recent years, increasing evidence has shown that circRNAs have potential in the diagnosis and treatment of tumors. Notably, circRNAs are conserved across species, are stably expressed in exosomes, plasma and saliva, and can promote cancer and chemotherapy resistance (45,50). Specific patterns of circRNA expression have been reported to be associated with tumor development and patient prognosis, indicating that they can serve as potential diagnostic and prognostic biomarkers (51). Previous studies have reported that a number of circRNAs, such as circ-MYBL2 (52), hsa\_circ\_0004277 (53) and circPVT1 (54), are abnormally expressed in AML. Alterations in circPVT1 can lead to amplification of the downstream oncogene MYC, and overexpression of MYC is associated with prognosis in AML (54). The present study revealed that circPVT1 expression was significantly upregulated in patients with AML and in AML cells, which was consistent with previous findings (23).

These findings suggested that circPVT1 may be a regulator of AML progression. However, few studies have investigated the mechanism of circPVT1 in AML (23,24).

MEF2 family members (MEF2A, 2B, 2C and 2D) serve key regulatory roles in AML progression (55,56). MEF2A is a well-known transcription factor that regulates the expression of numerous genes. It has previously been shown that MEF2A can be activated by TGF- $\beta$  through the upregulation of MMP10, which affects the ability of TGF- $\beta$  to induce breast cancer metastasis (57). In ovarian cancer, MEF2A is thought to be one of the transcription factors involved in tumorigenesis in response to norepinephrine (58). It has also been reported that MEF2A can bind to the promoter region of lncHCP5, upregulate the expression of lncHCP5 and affect the progression of gastric cancer (29). In addition, the transcription of circRNAs can be influenced by transcription factors (59). At present, to the best of our knowledge, there are no reports on the role of MEF2A transcription in regulating circPVT1 expression in disease. In the present study, through bioinformatics analysis, it was revealed that the transcription factor MEF2A could specifically bind to the circPVT1 promoter region with high affinity, which may significantly increase circPVT1 promoter activity. In addition, the overexpression of MEF2A in the AML cell lines NB4 and HL-60 significantly promoted the expression of circPVT1. Western blotting, CCK-8 assay and flow cytometry revealed that MEF2A overexpression significantly inhibited the expression of the proapoptotic proteins caspase-3 and Bax, enhanced the expression of the antiapoptotic protein Bcl-2, promoted the viability of NB4 and HL-60 cells, and inhibited their apoptosis. Moreover, EMT serves a key role in tumor progression, and the expression of E-cadherin is decreased, whereas the expression levels of N-cadherin, vimentin and fibronectin are upregulated during EMT (46). The current study revealed that MEF2A overexpression promoted EMT in AML cells. Therefore, it was hypothesized that MEF2A may affect the AML process by increasing circPVT1 expression.

There is growing evidence that circRNAs serve a functional role in a variety of biological processes, primarily by acting as miRNA sponges and ceRNAs (60). Through bioinformatics analysis, dual-luciferase reporter gene and Ago2-RIP assays, it was revealed that circPVT1 may have a targeted binding relationship with miR-455-3p. miR-455, a family of miRNAs closely related to several biological processes, has been shown to be clearly dysregulated in various human tumors, and is involved in the occurrence and progression of multiple malignancies (61-63). miR-455-3p is a member of the miR-455 family, and is involved in the occurrence and development of various malignant tumors. A previous study confirmed that miR-455-3p can promote the invasion and migration of triple-negative breast cancer by targeting the tumor suppressor EI24 (39). By contrast, miR-455-3p can act as a tumor inhibitor by targeting hTERT in melanoma A375 cells (40). In addition, transfection of a miR-455-3p mimic has been reported to inhibit the viability of AML cells (34). These findings suggested that miR-455-3p serves an important role in AML progression; however, studies on the regulatory mechanism of miR-455-3p in AML are limited. The present study demonstrated that the relative expression of miR-455-3p in the serum of patients with AML was decreased, and low expression of miR-455-3p was associated with the malignant

progression of AML cells, suggesting that miR-455-3p may act as a tumor suppressor in AML. The results also revealed that circPVT1 and miR-455-3p had a negative targeting relationship. Knocking down circPVT1 significantly inhibited the viability and EMT of NB4 and HL-60 cells, and promoted their apoptosis, whereas knocking down miR-455-3p promoted cell viability and EMT, and inhibited apoptosis. In summary, miR-455-3p may have a unique amelioratory function in AML by inhibiting cell viability. Therefore, miR-455-3p may serve as a potential biomarker for the treatment of AML.

The biological function of circRNAs as ceRNAs mainly depends on the downstream target mRNAs of miRNAs (29). Through bioinformatics analysis, it was revealed that MCL1 was a downstream target of miR-455-3p, and the interaction between miR-455-3p and MCL1 was confirmed by dual-luciferase reporter gene and Ago2-RIP assays. The current study revealed that MCL1 was positively correlated with circPVT1 and negatively correlated with miR-455-3p. MCL1 is a member of the Bcl-2 protein family with significant functions in regulating cellular metabolism and cancer progression (64). It has been shown that circHIPK3 can promote the proliferation and invasion of prostate cancer cells by sponging miR-193a-3p and regulating MCL1 expression (65). Li *et al* (47) reported that MCL1 upregulation was a common event in Chinese patients with *de novo* AML, which indicated that MCL1 may be associated with poor prognosis in patients with AML and can be used for disease surveillance. In addition, Lu *et al* (48) reported that miR-181b could improve the drug resistance of AML cells by decreasing the levels of MCL1. The present results revealed that the expression of MCL1 in the plasma of patients with AML was significantly upregulated. Furthermore, MCL1 knockdown weakened the effect of miR-455-3p knockdown, inhibited cell viability and EMT, and promoted cell apoptosis. To the best of our knowledge, the present study is the first to demonstrate that miR-455-3p interacts with MCL1 to influence the progression of AML. These findings provide a new theoretical basis for the treatment of AML.

Notably, the present study has limitations. First, the study only investigated the role of the MEF2A/circPVT1/miR-455-3p/MCL1 molecular axis in AML progression through *in vitro* experiments, and *in vivo* animal experiments are needed to further verify the role of this molecular axis. Second, miR-455-3p is not the only downstream target of circPVT1, and additional studies are needed to further explore the role of more miRNAs in AML and to develop more potential molecular therapeutic targets for AML. In addition, methylation of CpG islands has an important role in gene regulation. There are often differences in CpG island methylation between tumor cells and normal cells, and CpG island methylation is a common mechanism of gene inactivation in tumor cells, with AML samples often exhibiting very high methylation levels (66,67). However, whether the expression levels of circPVT1 are affected by the methylation of CpG islands in its promoter region, and whether this affects the AML process, requires further study.

In conclusion, to the best of our knowledge, the present study was the first to demonstrate that MEF2A, a transcription factor for circPVT1, could significantly promote the malignant progression of AML cells. Notably, circPVT1

knockdown inhibited the malignant progression of AML cells through the miR-455-3p/MCL1 axis. The identification of the circPVT1/miR-455-3p/MCL1 molecular axis may expand understanding of the underlying mechanisms of AML progression. Therefore, circPVT1 could be considered a diagnostic biomarker or a molecular therapeutic target for AML, and targeting the circPVT1/miR-455-3p/MCL1 molecular axis may provide novel therapeutic strategies for AML.

#### Acknowledgments

Not applicable.

#### Funding

The present study was supported by the ‘Xingdian Talents’ Support Project of Yunnan Province (grant nos. RLMY20220006 and RLMY20200020) and the Kunming-Medical Joint Special Project of the Yunnan Provincial Department of Science and Technology (grant no. 202201AY070001-058).

#### Availability of data and materials

The data generated in the present study may be requested from the corresponding author.

#### Authors' contributions

KW, MS and YL conceptualized the study. KW, MS, YZ and JY designed the experimental methods. YL, YZ and BN used software to analyze data. CG and XM validated the data. KW and XM carried out formal analysis. KW, MS, YZ and JY conducted the investigation. MS, YZ and JY provided resources. CG, LL and SC were responsible for acquisition of data. BN and SL were responsible for interpretation of data. KW, SC and YL were responsible for writing the original draft. KW, LL and SL reviewed and edited the manuscript. YL and SL edited the figures. SL, YZ, JY and MS supervised the study. MS, JY and SL received funding. KW, JY and MS confirm the authenticity of all the raw data. All authors read and approved the final version of the manuscript.

#### Ethics approval and consent to participate

The study was approved by the Ethics Committee of The First Affiliated Hospital of Kunming Medical University (approval no. L-10; approval date, March 8, 2021) and was conducted in accordance with The Declaration of Helsinki. The participants provided written informed consent prior to taking part in the study. The guardian of the 16-year-old patient also provided consent.

#### Patient consent for publication

Not applicable.

#### Competing interests

The authors declare that they have no competing interests.

#### References

- Juliussen G, Lazarevic V, Hörstedt AS, Hagberg O and Höglund M; Swedish Acute Leukemia Registry Group: Acute myeloid leukemia in the real world: Why population-based registries are needed. *Blood* 119: 3890-3899, 2012.
- El Hussein S, Wang SA, Pemmaraju N, Khoury JD and Loghavi S: Chronic Myelomonocytic leukemia: Hematopathology perspective. *J Immunother Precis Oncol* 4: 142-149, 2021.
- Lonetti A, Pession A and Masetti R: Targeted therapies for pediatric AML: Gaps and perspective. *Front Pediatr* 7: 463, 2019.
- Anguille S, Van Tendeloo VF and Berneman ZN: Leukemia-associated antigens and their relevance to the immunotherapy of acute myeloid leukemia. *Leukemia* 26: 2186-2196, 2012.
- Tsykunova G, Reikvam H, Hovland R and Bruserud Ø: The surface molecule signature of primary human acute myeloid leukemia (AML) cells is highly associated with NPM1 mutation status. *Leukemia* 26: 557-559, 2012.
- Hope KJ, Jin L and Dick JE: Acute myeloid leukemia originates from a hierarchy of leukemic stem cell classes that differ in self-renewal capacity. *Nat Immunol* 5: 738-743, 2004.
- Song X, Peng Y, Wang X, Chen Y, Jin L, Yang T, Qian M, Ni W, Tong X and Lan J: Incidence, survival, and risk factors for adults with acute myeloid leukemia not otherwise specified and acute myeloid leukemia with recurrent genetic abnormalities: Analysis of the surveillance, epidemiology, and end results (SEER) database, 2001-2013. *Acta Haematol* 139: 115-127, 2018.
- Li S, Zhu Y, Liang Z, Wang X, Meng S, Xu X, Xu X, Wu J, Ji A, Hu Z, *et al*: Correction: Up-regulation of p16 by miR-877-3p inhibits proliferation of bladder cancer. *Oncotarget* 10: 684, 2019.
- Guerra VA, Dinardo C and Konopleva M: Venetoclax-based therapies for acute myeloid leukemia. *Best Pract Res Clin Haematol* 32: 145-153, 2019.
- Pan B, Qin J, Liu X, He B, Wang X, Pan Y, Sun H, Xu T, Xu M, Chen X, *et al*: Identification of serum exosomal hsa-circ-0004771 as a novel diagnostic biomarker of colorectal cancer. *Front Genet* 10: 1096, 2019.
- Jamal M, Song T, Chen B, Faisal M, Hong Z, Xie T, Wu Y, Pan S, Yin Q, Shao L and Zhang Q: Recent progress on circular RNA research in acute myeloid leukemia. *Front Oncol* 9: 1108, 2019.
- Yin Y, Long J, He Q, Li Y, Liao Y, He P and Zhu W: Emerging roles of circRNA in formation and progression of cancer. *J Cancer* 10: 5015-5021, 2019.
- Yang Y, Yujiao W, Fang W, Linhui Y, Ziqi G, Zhichen W, Zirui W and Shengwang W: The roles of miRNA, lncRNA and circRNA in the development of osteoporosis. *Biol Res* 53: 40, 2020.
- Shafabakhsh R, Mirhosseini N, Chaichian S, Moazzami B, Mahdizadeh Z and Asemi Z: Could circRNA be a new biomarker for pre-eclampsia? *Mol Reprod Dev* 86: 1773-1780, 2019.
- Chen J, Li Y, Zheng Q, Bao C, He J, Chen B, Lyu D, Zheng B, Xu Y, Long Z, *et al*: Circular RNA profile identifies circPVT1 as a proliferative factor and prognostic marker in gastric cancer. *Cancer Lett* 388: 208-219, 2017.
- Zhang J, Liu H, Hou L, Wang G, Zhang R, Huang Y, Chen X and Zhu J: Circular RNA\_LARP4 inhibits cell proliferation and invasion of gastric cancer by sponging miR-424-5p and regulating LATS1 expression. *Mol Cancer* 16: 151, 2017.
- Li P, Chen H, Chen S, Mo X, Li T, Xiao B, Yu R and Guo J: Circular RNA 0000096 affects cell growth and migration in gastric cancer. *Br J Cancer* 116: 626-633, 2017.
- Wei CB, Tao K, Jiang R, Zhou LD, Zhang QH and Yuan CS: Quercetin protects mouse liver against triptolide-induced hepatic injury by restoring Th17/Treg balance through Tim-3 and TLR4-MyD88-NF-κB pathway. *Int Immunopharmacol* 53: 73-82, 2017.
- Liu YP, Wan J, Long F, Tian J and Zhang C: circPVT1 facilitates invasion and metastasis by regulating miR-205-5p/c-FLIP axis in osteosarcoma. *Cancer Manag Res* 12: 1229-1240, 2020.
- Zheng F and Xu R: CircPVT1 contributes to chemotherapy resistance of lung adenocarcinoma through miR-145-5p/ABCC1 axis. *Biomed Pharmacother* 124: 109828, 2020.
- Wang J, Huang K, Shi L, Zhang Q and Zhang S: CircPVT1 promoted the progression of breast cancer by regulating MiR-29a-3p-Mediated AGR2-HIF-1α pathway. *Cancer Manag Res* 12: 11477-11490, 2020.

22. Chen T and Chen F: The role of circular RNA plasmacytoma variant translocation 1 as a biomarker for prognostication of acute myeloid leukemia. *Hematology* 26: 1018-1024, 2021.
23. Ghetti M, Vannini I, Bochicchio MT, Azzali I, Ledda L, Marconi G, Melloni M, Fabbri F, Rondoni M, Chicchi R, *et al*: Uncovering the expression of circPVT1 in the extracellular vesicles of acute myeloid leukemia patients. *Biomed Pharmacother* 165: 115235, 2023.
24. Sheng XF, Hong LL, Fan L, Zhang Y, Chen KL, Mu J, Shen SY and Zhuang HF: Circular RNA PVT1 regulates cell proliferation, migration, and apoptosis by stabilizing c-Myc and downstream target CXCR4 expression in acute myeloid leukemia. *Turk J Haematol* 40: 82-91, 2023.
25. Ryan RJH, Drier Y, Whitton H, Cotton MJ, Kaur J, Issner R, Gillespie S, Epstein CB, Nardi V, Sohani AR, *et al*: Detection of enhancer-associated rearrangements reveals mechanisms of oncogene dysregulation in B-cell lymphoma. *Cancer Discov* 5: 1058-1071, 2015.
26. Brown FC, Still E, Koche RP, Yim CY, Takao S, Cifani P, Reed C, Gunasekera S, Ficarro SB, Romanienko P, *et al*: MEF2C phosphorylation is required for chemotherapy resistance in acute myeloid leukemia. *Cancer Discov* 8: 478-497, 2018.
27. Ma L, Liu J, Liu L, Duan G, Wang Q, Xu Y, Xia F, Shan J, Shen J, Yang Z, *et al*: Overexpression of the transcription factor MEF2D in hepatocellular carcinoma sustains malignant character by suppressing G2-M transition genes. *Cancer Res* 74: 1452-1462, 2014.
28. Xiang J, Sun H, Su L, Liu L, Shan J, Shen J, Yang Z, Chen J, Zhong X, Avila MA, *et al*: Myocyte enhancer factor 2D promotes colorectal cancer angiogenesis downstream of hypoxia-inducible factor 1 $\alpha$ . *Cancer Lett* 400: 117-126, 2017.
29. Chen W, Zhang K, Yang Y, Guo Z, Wang X, Teng B, Zhao Q, Huang C and Qiu Z: MEF2A-mediated lncRNA HCP5 inhibits gastric cancer progression via MiR-106b-5p/p21 axis. *Int J Biol Sci* 17: 623-634, 2021.
30. Xiao Q, Gan Y, Li Y, Fan L, Liu J, Lu P, Liu J, Chen A, Shu G and Yin G: MEF2A transcriptionally upregulates the expression of ZEB2 and CTNBN1 in colorectal cancer to promote tumor progression. *Oncogene* 40: 3364-3377, 2021.
31. Xia L, Nie T, Lu F, Huang L, Shi X, Ren D, Lu J, Li X, Xu T, Cui B, *et al*: Direct regulation of FNIP1 and FNIP2 by MEF2 sustains MTORC1 activation and tumor progression in pancreatic cancer. *Autophagy* 20: 505-524, 2024.
32. Hansen TB, Jensen TI, Clausen BH, Bramsen JB, Finsen B, Damgaard CK and Kjems J: Natural RNA circles function as efficient microRNA sponges. *Nature* 495: 384-388, 2013.
33. Yi J, Wang L, Hu GS, Zhang YY, Du J, Ding JC, Ji X, Shen HF, Huang HH, Ye F and Liu W: CircPVT1 promotes ER-positive breast tumorigenesis and drug resistance by targeting ESR1 and MAVS. *EMBO J* 42: e112408, 2023.
34. Xie Y, Tan L, Wu K, Li D and Li C: MiR-455-3p mediates PPAR $\alpha$  through UBN2 to promote apoptosis and autophagy in acute myeloid leukemia cells. *Exp Hematol* 128: 77-88, 2023.
35. Zhan T, Zhu Q, Han Z, Tan J, Liu M, Liu W, Chen W, Chen X, Chen X, Deng J, *et al*: miR-455-3p functions as a tumor suppressor by restraining Wnt/ $\beta$ -catenin signaling via TAZ in pancreatic cancer. *Cancer Manag Res* 12: 1483-1492, 2020.
36. Ni X, Ding Y, Yuan H, Shao J, Yan Y, Guo R, Luan W and Xu M: Long non-coding RNA ZEB1-AS1 promotes colon adenocarcinoma malignant progression via miR-455-3p/PAK2 axis. *Cell Prolif* 53: e12723, 2020.
37. Liu A, Zhu J, Wu G, Cao L, Tan Z, Zhang S, Jiang L, Wu J, Li M, Song L and Li J: Correction to: Antagonizing miR-455-3p inhibits chemoresistance and aggressiveness in esophageal squamous cell carcinoma. *Mol Cancer* 20: 152, 2021.
38. Gao X, Zhao H, Diao C, Wang X, Xie Y, Liu Y, Han J and Zhang M: miR-455-3p serves as prognostic factor and regulates the proliferation and migration of non-small cell lung cancer through targeting HOXB5. *Biochem Biophys Res Commun* 495: 1074-1080, 2018.
39. Li Z, Meng Q, Pan A, Wu X, Cui J, Wang Y and Li L: MicroRNA-455-3p promotes invasion and migration in triple negative breast cancer by targeting tumor suppressor EI24. *Oncotarget* 8: 19455-19466, 2017.
40. Chai L, Kang XJ, Sun ZZ, Zeng MF, Yu SR, Ding Y, Liang JQ, Li TT and Zhao J: MiR-497-5p, miR-195-5p and miR-455-3p function as tumor suppressors by targeting hTERT in melanoma A375 cells. *Cancer Manag Res* 10: 989-1003, 2018.
41. Ryu S, Park HS, Kim SM, Im K, Kim JA, Hwang SM, Yoon SS and Lee DS: Shifting of erythroleukemia to myelodysplastic syndrome according to the revised WHO classification: Biologic and cytogenetic features of shifted erythroleukemia. *Leuk Res* 70: 13-19, 2018.
42. Li LC and Dahiya R: MethPrimer: Designing primers for methylation PCRs. *Bioinformatics* 18: 1427-1431, 2002.
43. Livak KJ and Schmittgen TD: Analysis of relative gene expression data using real-time quantitative PCR and the 2(-Delta Delta C(T)) method. *Methods* 25: 402-408, 2001.
44. Li L, Lv G, Wang B and Kuang L: The role of lncRNA XIST/miR-211 axis in modulating the proliferation and apoptosis of osteoarthritis chondrocytes through CXCR4 and MAPK signaling. *Biochem Biophys Res Commun* 503: 2555-2562, 2018.
45. Li S, Liu F, Zheng K, Wang W, Qiu E, Pei Y, Wang S, Zhang J and Zhang X: CircDOCK1 promotes the tumorigenesis and cisplatin resistance of osteogenic sarcoma via the miR-339-3p/IGF1R axis. *Mol Cancer* 20: 161, 2021.
46. Matoba R, Morizane Y, Shiode Y, Hirano M, Doi S, Toshima S, Araki R, Hosogi M, Yonezawa T and Shiraga F: Suppressive effect of AMP-activated protein kinase on the epithelial-mesenchymal transition in retinal pigment epithelial cells. *PLoS One* 12: e0181481, 2017.
47. Li XX, Zhou JD, Wen XM, Zhang TJ, Wu DH, Deng ZQ, Zhang ZH, Lian XY, He PF, Yao XY, *et al*: Increased MCL-1 expression predicts poor prognosis and disease recurrence in acute myeloid leukemia. *Onco Targets Ther* 12: 3295-3304, 2019.
48. Lu F, Zhang J, Ji M, Li P, Du Y, Wang H, Zang S, Ma D, Sun X and Ji C: miR-181b increases drug sensitivity in acute myeloid leukemia via targeting HMGB1 and Mcl-1. *Int J Oncol* 45: 383-392, 2014.
49. Xu M and Li S: The opportunities and challenges of using PD-1/PD-L1 inhibitors for leukemia treatment. *Cancer Lett* 593: 216969, 2024.
50. Guo X, Gao C, Yang DH and Li S: Exosomal circular RNAs: A chief culprit in cancer chemotherapy resistance. *Drug Resist Updat* 67: 100937, 2023.
51. Liu Q and Li S: Exosomal circRNAs: Novel biomarkers and therapeutic targets for urinary tumors. *Cancer Lett* 588: 216759, 2024.
52. Sun YM, Wang WT, Zeng ZC, Chen TQ, Han C, Pan Q, Huang W, Fang K, Sun LY, Zhou YF, *et al*: circMYBL2, a circRNA from MYBL2, regulates FLT3 translation by recruiting PTBP1 to promote FLT3-ITD AML progression. *Blood* 134: 1533-1546, 2019.
53. Li W, Zhong C, Jiao J, Li P, Cui B, Ji C and Ma D: Characterization of hsa\_circ\_0004277 as a new biomarker for acute myeloid leukemia via circular RNA profile and bioinformatics analysis. *Int J Mol Sci* 18: 597, 2017.
54. Hu J, Han Q, Gu Y, Ma J, Mcgrath M, Qiao F, Chen B, Song C and Ge Z: Circular RNA PVT1 expression and its roles in acute lymphoblastic leukemia. *Epigenomics* 10: 723-732, 2018.
55. Tarumoto Y, Lin S, Wang J, Milazzo JP, Xu Y, Lu B, Yang Z, Wei Y, Polyanskaya S, Wunderlich M, *et al*: Salt-inducible kinase inhibition suppresses acute myeloid leukemia progression in vivo. *Blood* 135: 56-70, 2020.
56. Zhao L, Zhang P, Galbo PM, Zhou X, Aryal S, Qiu S, Zhang H, Zhou Y, Li C, Zheng D, *et al*: Transcription factor MEF2D is required for the maintenance of MLL-rearranged acute myeloid leukemia. *Blood Adv* 5: 4727-4740, 2021.
57. Ishikawa F, Miyoshi H, Nose K and Shibamura M: Transcriptional induction of MMP-10 by TGF-beta, mediated by activation of MEF2A and downregulation of class IIa HDACs. *Oncogene* 29: 909-919, 2010.
58. Gjyshi A, Dash S, Cen L, Cheng CH, Zhang C, Yoder SJ, Teer JK, Armaiz-Pena GN and Monteiro ANA: Early transcriptional response of human ovarian and fallopian tube surface epithelial cells to norepinephrine. *Sci Rep* 8: 8291, 2018.
59. Huang S, Li X, Zheng H, Si X, Li B, Wei G, Li C, Chen Y, Chen Y, Liao W, *et al*: Loss of super-enhancer-regulated circRNA Nfix induces cardiac regeneration after myocardial infarction in adult mice. *Circulation* 139: 2857-2876, 2019.
60. Yang X, Han F, Hu X, Li G, Wu H, Can C, Wei Y, Liu J, Wang R, Jia W, *et al*: EIF4A3-induced Circ\_0001187 facilitates AML suppression through promoting ubiquitin-proteasomal degradation of METTL3 and decreasing m6A modification level mediated by miR-499a-5p/RNF113A pathway. *Biomark Res* 11: 59, 2023.
61. Sand M, Skrygan M, Sand D, Georgas D, Hahn SA, Gambichler T, Altmeyer P and Bechara FG: Expression of microRNAs in basal cell carcinoma. *Br J Dermatol* 167: 847-855, 2012.



62. Zhang Z, Hou C, Meng F, Zhao X, Zhang Z, Huang G, Chen W, Fu M and Liao W: MiR-455-3p regulates early chondrogenic differentiation via inhibiting Runx2. *FEBS Lett* 589: 3671-3678, 2015.
63. Boisen MK, Dehlendorff C, Linnemann D, Nielsen BS, Larsen JS, Osterlind K, Nielsen SE, Tarpgaard LS, Qvortrup C, Pfeiffer P, *et al*: Tissue microRNAs as predictors of outcome in patients with metastatic colorectal cancer treated with first line capecitabine and oxaliplatin with or without bevacizumab. *PLoS One* 9: e109430, 2014.
64. Williams MM, Lee L, Hicks DJ, Joly MM, Elion D, Rahman B, Mckernan C, Sanchez V, Balko JM, Stricker T, *et al*: Key Survival factor, Mcl-1, correlates with sensitivity to combined Bcl-2/Bcl-xL blockade. *Mol Cancer Res* 15: 259-268, 2017.
65. Chen D, Lu X, Yang F and Xing N: Circular RNA circHIPK3 promotes cell proliferation and invasion of prostate cancer by sponging miR-193a-3p and regulating MCL1 expression. *Cancer Manag Res* 11: 1415-1423, 2019.
66. Strathdee G, Sim A, Soutar R, Holyoake TL and Brown R: HOXA5 is targeted by cell-type-specific CpG island methylation in normal cells and during the development of acute myeloid leukaemia. *Carcinogenesis* 28: 299-309, 2007.
67. Zhou H, Zhang Q, Huang W, He C, Zhou C, Zhou J and Ning Y: Epigenetic silencing of ZCCHC10 by the lncRNA SNHG1 promotes progression and venetoclax resistance of acute myeloid leukemia. *Int J Oncol* 62: 64, 2023.



Copyright © 2024 Wu et al. This work is licensed under a Creative Commons Attribution-NonCommercial-NoDerivatives 4.0 International (CC BY-NC-ND 4.0) License.